EPJ manuscript No.
(will be inserted by the editor)

Multi-time-scale synchronization and information processing in bursting neuron networks

T. Pereira[1,a], M.S. Baptista[2], and J. Kurths[1]

[1] Universität Potsdam, Institut für Physik Am Neuen Palais 10, D-14469 Potsdam, Deutschland.
[2] Max-Planck-Institut für Physik Komplexer Systeme, Nöthnitzer Str. 38, D-01187 Dresden, Deutschland.

Abstract. We analyze the effect of synchronization in networks of chemically coupled multi-time-scale (spiking-bursting) neurons on the process of information transmission within the network. Although, synchronization occurs first in the slow time-scale (burst) and then in the fast time-scale (spike), we show that information can be transmitted with low probability of errors in both time scales when the bursts become synchronized. Furthermore, we show that for networks of non-identical multi-time-scales neurons, complete synchronization is no longer possible, but instead burst phase synchronization. Our analysis shows that clusters of burst phase synchronized neurons are very likely to appear in a network for parameters far smaller than the ones for which the onset of burst phase synchronization in the whole network happens

1 Introduction

Certain neurons in the brain exhibit a multi-time-scale behavior called spike-burst activity, a recurrent transition between a fast (spikes) and a slow (rest) dynamics [1,2]. The spiking dynamics consists of the action potentials [3], result of the exchange of fast currents such as K^+ of the external media with the neuron. On the other hand, the neuron may also exchange slow currents such as Ca^{+2}, which inhibits the occurrence of spikes generating the slow dynamics almost a rest state, the hyperpolarization. The typical membrane potential of a spiking-bursting neuron consists of bursts of multiple spikes followed by a rest state hyperpolarization.

These neurons have a great importance in different aspects of brain function such as movement control and cognition [4–6]. There are evidences that synchronization may be related to a series of processes in the brain. Experimental observations of neuron networks present synchronized oscillations in response to sensory stimuli in a variety of brain areas [7,10,8,9]. In the human perception process, the gamma wave is globally synchronized in space and time [7]. Experiments with fear-conditioned mice have shown the synchronized activity of the theta wave in the amygdalohippocampal network[10]. Nevertheless, the onset of synchronization in a network may also lead to some diseases, e.g. Parkinson disease [11] and epilepsy [12].

Interestingly, different types of synchronization may take place in multi-time-scale neurons. They may present bursting synchronization. And, a situation where both spikes and bursts are synchronous. Typically, bursting synchronization arises for lower coupling strengths, whereas complete synchrony requires a stronger coupling.

The coupling between neurons may occur via two different types of synapses, the electrical or chemical synapses [3]. In the former case, the coupling occurs through gap junctions and its

[a] e-mail: tiagops@agnld.uni-potsdam.de

strength depends linearly on the difference between the membrane potentials. In order to realize this synaptic connection the neurons must be very close to each other. Therefore, electrical networks with long range connections are not possible, but one may find small arrays/rings of locally electrically coupled neurons. In the chemical case, the synapse is mediated by neurotransmitters and the connection occurs between the dendrites and the axons, therefore, it allows long range connections, which generates complex network structures.

These synaptic inputs and external stimuli arriving in the network must be spread to many areas or neurons in the network. *How well these stimuli could be spread?* This question is a key point towards a better understanding of the brain and neuron network functioning. It concerns both the architecture of the network and the dynamical behavior of the nodes.

In order to spread the stimuli the brain must first encode the information. The code used may depend on the particular dynamical behavior of the oscillators the network is composed of. It is generally agreed that, in certain situations, the brain encodes information using either the time between spikes or between bursts [13–15]. In such a case, synchronization plays a role in the information transmission, since synchronization may improve the timing between spikes or bursts. Thus, the study of synchronization and desynchronization of neuronal spike-burst behaviors from biophysical models may be helpful to understand further the information processing in the brain.

We analyze the effect of synchronization on the information flow. We show that the information capacity depends on: (*i*) how the code is defined, whether one uses the burst or the spikes; (*ii*) the synchronization level. Synchronization may occurs in distinct time-scales, which can be suitably used for information transmission. Moreover, we show that clusters of synchronization may appear on the network before the onset of synchronization in the network, which provides a good environment for information transmission without the enhancement of a collective behavior in a massive population of neurons.

2 Synchronization and Information

The classical idea of synchronization states that one can understand two synchronized oscillators by studying only one of them, once they present the same dynamical behavior. This seems to be a rather old concept. Back in the 16th century, Spinoza, a Dutch philosopher, had shared this same idea, in a somewhat different context. In his work ethics [16] he states the following proposition: " *Things which have nothing in common cannot be understood, the one by means of the other; the conception of one does not involve the conception of the other,* " which captures the modern idea of synchronization [17]. Synchronization ought to imply a collapse of the overall evolution onto a subspace of the system attractor, reducing the dimensionality of the system.

Synchronization can be enhanced at different levels, that is, the constraints on which the synchronization appears. Those can be in the trajectory amplitude, requiring the amplitudes of both oscillators to be equal, giving place to complete synchronization [18–23]. Conversely, the constraint could also be in a function of the trajectory, the phase, giving place to phase synchronization (PS) [23,26,30,28,24,25,27,29]. In this case, one requires the phase difference between both oscillators to be finite for all times, while no constraint on the trajectory amplitude is imposed. The former case requires relatively strong coupling strengths, whereas, in general, the later can arise for very small coupling strengths.

These different types of synchronization may arise depending on the nature of the oscillator and on the coupling properties. Given two identical oscillators $\mathbf{x}_i$ and $\mathbf{x}_j$ coupled properly, for strong enough coupling strengths, CS can be achieved. This means that both trajectories present the same behavior:

$$\lim_{t\to\infty} |\mathbf{x}_i(t) - \mathbf{x}_j(t)| = 0. \tag{1}$$

Synchronization in this case is associated with a transition of the largest transverse Lyapunov exponent of the subspace $\mathbf{x}_i = \mathbf{x}_j$, also known as synchronization manifold [21,22], from positive to negative values. In general, complete synchronization is only possible if the interacting oscillators are identical. If their parameters mismatch the states can be close $\mathbf{x}_i \approx \mathbf{x}_j$, but not equal. For non-identical oscillators, other types of synchronization can appear [23,22]. Here

we focus on PS. Denoting, $\vartheta_{i,j}(t)$ the phase of $\mathbf{x}_{i,j}$ the condition for phase synchronization is given by:

$$|n\vartheta_i(t) - m\vartheta_j(t)| \leq \varrho, \tag{2}$$

where n and m are integers, and the inequality must hold for all times, with ϱ being a finite number. Herein, we consider the case where $n = m = 1$, in other words $1:1$ PS. The study of PS has shown its relevance to important technological problems such as communication with chaos [31,32], new insights into the collective behavior in networks of coupled chaotic oscillators [33,34], pattern formation [35,23], Parkinson disease [11], epilepsy [12], as well as behavioral activities [36].

2.1 Synchronization detection

The detection of CS is straightforward, due to the simple geometric constraints of the synchronization manifold. One only requires Eq. (1) to be valid. Thus, for detection and analysis purposes one may look at the amount $\boldsymbol{\xi}_{ij} = \mathbf{x}_i(t) - \mathbf{x}_j(t)$; if it converges to zero in the limit of large times, then complete synchronization is present. In a network composed of N oscillators, one may analyze all transverse directions $\boldsymbol{\xi}_{ij}$, where $i, j \in 1, 2, \cdots, N$. In practice one may analyze only the behavior of the largest transversal exponent associated with the synchronization manifold.

The detection of PS is more problematic. In order to state the existence of PS, one has to introduce a phase $\phi(t)$ for the chaotic oscillator, what is not straightforward. Even though the phase is expected to exist to a general attractor, due to the existence of the zero Lyapunov exponent [21,23], its explicit calculation, for a general oscillator, may be impossible. Actually, even for the simple case of coherent attractors, the phase can be defined in different ways, each one being chosen according to the particular case studied [37,38]. The calculation becomes even harder if the oscillators are non-coherent, e.g., the funnel oscillator [23] or have no proper rotation [32], as an example a double-scroll attractor. Therefore, in order to present a general approach to detect PS, with practical applications, we must overcome the need of a phase.

We have shown that PS implies the existence of localized sets of the attractor [39], which is generated by the observations of the attractor [40–44]. The basic idea consists in the conditional observation of one oscillator constrained to an event occurrence in the other oscillator.

The event definition can be arbitrary. The only constraint is that it must be typical. Therefore, the event could be a local maximum/minimum, the crossing of a dynamical variable with a threshold, the entrance in an ε-ball, and so on. We also suppose that there is a function phase ϕ_i, in such a way that $\dot{\phi}_i = \Omega_i$ (an instantaneous frequency), where Ω_i is continuous and $0 < \Omega_i \leq \Upsilon$. Under such hypotheses, we can state that: *Given any typical event, with positive measure, in the oscillator $\Sigma_{i,j}$, generating the times $(t_{i,j}^k)_{k\in\mathbb{N}}$, if there is PS the observation of $\mathbf{x}_i$ at $(t_j^k)_{k\in\mathbb{N}}$ generates a localized set $\mathcal{D}_i$.*

2.2 Information

In this section, we analyze the relationship between the sets $\mathcal{D}$ and the capacity of information transmission between coupled oscillators. In order to proceed with such an analysis, we may assume that the oscillators are identical or nearly identical, such that the synchronized trajectories are close to the synchronization manifold $\mathbf{x}_j = \mathbf{x}_i$.

The amount of information that two systems $\mathbf{x}_i$ and $\mathbf{x}_j$ can exchange is given by the mutual information [45]:

$$I(\mathbf{x}_i, \mathbf{x}_j) = H(\mathbf{x}_i) - H(\mathbf{x}_i|\mathbf{x}_j), \tag{3}$$

where $H(\mathbf{x}_i)$ is the entropy of the oscillator $\mathbf{x}_i$ and $H(\mathbf{x}_i|\mathbf{x}_j)$ is the conditional entropy between $\mathbf{x}_i$ and $\mathbf{x}_j$, which measures the ambiguity of the received signal, roughly speaking the errors in the transmission.

As pointed out in Ref. [46] the mutual information can also be estimated by means of the conditional exponents associated with the synchronization manifold. In this case, the mutual information is given by:

$$I(\mathbf{x}_i, \mathbf{x}_j) = \sum \lambda_{\|}^{+} - \sum \lambda_{\perp}^{+}, \tag{4}$$

where $\lambda_{\|}^{+}$ are the positive conditional Lyapunov exponents associated to the synchronization manifold, the information produced by the synchronous trajectories, and $\lambda_{\perp}^{+}$ are the positive conditional Lyapunov exponents transversal to the synchronization manifold, related with the errors in the information transmission. In PS, $\lambda_{\perp}^{+}$ can be small, which means that one can exchange information with a low probability of errors. So, PS creates a channel for reliable information exchanging [46]. In order to estimate the upper bound for the information capacity, we note that, in general, $\sum \lambda_{\|}^{+} \leq \sum \lambda^{+}$, where λ^{+} are the positive Lyapunov exponents. Thus $I(\mathbf{x}_i, \mathbf{x}_j) \leq \sum \lambda^{+} - \sum \lambda_{\perp}^{+}$. Now, we need to estimate $\lambda_{\perp}^{+}$, what can be done directly from the localized sets.

The conditional transversal exponent can be estimated from the localized sets by a simple geometric analysis. At the time t_j^k the oscillator Σ_j reaches the Poincaré plane at $\mathbf{x}_j^*$ while the oscillator Σ_i is at $\mathbf{x}_i^k = \mathbf{x}_i(t_j^k)$. The initial distance between the trajectories is $\Delta\mathbf{x}_{ij} = \mathbf{x}_j^* - \mathbf{x}_i^k$. This distance evolves until the time t_i^k when the oscillator Σ_i reaches the Poincaré plane at $\mathbf{x}_i^*$, while the trajectory of Σ_j is at $\mathbf{x}_j^k = \mathbf{x}_j(t_i^k)$. The new distance is $\Delta\tilde{\mathbf{x}}_{ij} = \mathbf{x}_i^* - \mathbf{x}_j^k$. Therefore, we have:

$$\Delta\tilde{\mathbf{x}}_{ij} = \Delta\mathbf{x}_{ij} e^{\lambda_{\perp}^{+}|t_i^k - t_j^k|}. \tag{5}$$

So, the local transversal exponent is given by:

$$\lambda_{\perp}^{+} = \lim_{N\to\infty} \frac{1}{N} \sum_{i=1}^{N} \frac{1}{|t_i^k - t_j^k|} \ell n \left| \frac{\mathbf{x}_i^* - \mathbf{x}_j^k}{\mathbf{x}_j^* - \mathbf{x}_i^k} \right|. \tag{6}$$

We only estimate the conditional exponent close to the Poincaré plane. Hence, if we change the Poincaré plane the conditional exponent may also change. This means that there are some events that carry more information than others. Note that the local conditional exponent gives less information than observing the full trajectory, because we ignore the dynamics apart from the Poincaré plane.

The rough idea is that the more synchronized the oscillators are, the more information they can exchange. In order to illustrate this idea, we consider two oscillators $\mathbf{x}_1$ and $\mathbf{x}_2$, coupled via a given function such that they may undergo a transition to CS. We introduce a signal in the trajectory of $\mathbf{x}_1$ and then we try to read off the signal in the trajectory of $\mathbf{x}_2$. We may have three regimes: (i) no synchronization; consider the decoupled oscillator, it is impossible to receive information about the signal in $\mathbf{x}_2$. (ii) an intermittent synchronization regime; we will be able to read off some parts of the signal introduced in $\mathbf{x}_1$. (iii) complete synchronization, suppose that the signal which has been introduced is not able to destroy synchronization; thus, all the signal (information) will be read off in $\mathbf{x}_2$. In a network, the connection between synchronization and information is less clear.

3 Spiking-Bursting Neurons

For our purposes, it is worthy to note that a multi-time-scale dynamical system, such as a spiking/bursting neuron, can be written in a singular perturbed form:

$$\begin{aligned} \dot{\mathbf{x}} &= \boldsymbol{F}(\mathbf{x}, \mathbf{z}), \\ \dot{\mathbf{z}} &= \mu \boldsymbol{G}(\mathbf{x}, \mathbf{z}), \end{aligned} \tag{7}$$

where $\mathbf{x}$ is the vector of fast variables, and $\mathbf{z}$ is a vector of slow variables. The fast variables are modulated by the slow ones. The value of $\mu \ll 1$ gives the ratio between the fast/slow time

scales. One can study the fast and slow subsystems separately to know exactly when each time scale becomes synchronous, and then, we can understand the effect of having a synchronous time-scale in the transmission of information. For now, let us consider two coupled bursting oscillators:

$$\begin{aligned}\dot{\mathbf{x}}_i &= \boldsymbol{F}(\mathbf{x}_i, \mathbf{z}_i) + g_{syn} \sum_j c_{ij} \mathbf{H}(\mathbf{x}_i, \mathbf{x}_j), \\ \dot{\mathbf{z}}_i &= \mu \boldsymbol{G}(\mathbf{x}_i, \mathbf{z}_i),\end{aligned} \tag{8}$$

where c_{ij} is the coupling matrix (2 by 2 for the case of two neurons). The parameter g_{syn} is the synapse strength, and $\mathbf{H}(\mathbf{x}_i, \mathbf{x}_j)$ is the coupling function. The synchronized motion in a hyperplane given by the constrains $\mathbf{x}_1 = \mathbf{x}_2 = \mathbf{x}$ and $\mathbf{z}_1 = \mathbf{z}_2 = \mathbf{z}$ defines the synchronization manifold. The analysis of stability of the synchronization manifold can predict whether there exist a synchronized solution. The behavior of the largest transverse Lyapunov exponent fully determines the linear stability of the synchronized solutions.

Herein, we consider the Hindmarsh-Rose neuron [47]. The dynamical variables are $\mathbf{x}_i = (x_i, y_i)^T$ and $\mathbf{z}_i = z_i$, and the equations $\boldsymbol{F}$ and $\boldsymbol{G}$ read:

$$\begin{aligned}\boldsymbol{F}(\mathbf{x}_i, \mathbf{z}_i) &= (f(\mathbf{x}, \mathbf{y}), g(\mathbf{x}, \mathbf{y}))^T = (y_i + a x_i^2 - x_i^3 - z_i + I_{ext}, 1 + b x_i^2 - y_i)^T, \\ \boldsymbol{G}(\mathbf{x}_i, \mathbf{y}_i) &= (\mu[s(x_i - x_0) - z_i]).\end{aligned} \tag{9}$$

The parameters are $a = 3, b = -5, x_0 = -1.6, \mu = 0.006$, and $s = 4$. We shall consider two different coupling functions (or synaptic connection), namely the electrical synapse, and the chemical one.

3.1 Electric Synapse

The coupling reads $\mathbf{H}(\mathbf{x}_i, \mathbf{x}_j) = \mathbf{H}(\mathbf{x}_j) = (\mathbf{x}_j, 0)^T$, $c_{ii} = -1$, and $c_{ij} = 1$ if $i \neq j$. In this case, the synchronized solution on the synchronization manifold takes the form:

$$\begin{aligned}\dot{x} &= y + a x^2 - x^3 - z + I_{ext}, \\ \dot{y} &= 1 + b x^2 - y, \\ \dot{z} &= \mu[s(x - x_0) - z].\end{aligned} \tag{10}$$

Note that since $\mathbf{x}_1 = \mathbf{x}_2$ and $\sum_j c_{ij} = 0$ the contribution of the coupling vanishes on the synchronization manifold. Let us consider $\boldsymbol{\xi} = \mathbf{x}_1 - \mathbf{x}_2 = (\xi, \eta)$, and $\boldsymbol{\zeta} = \mathbf{z}_1 - \mathbf{z}_2 = \zeta$. As a result we have:

$$\begin{aligned}\dot{\boldsymbol{\xi}} &= D_{\mathbf{x}} \boldsymbol{F}(\mathbf{x}, \mathbf{z}) \boldsymbol{\xi} + D_{\mathbf{z}} \boldsymbol{F}(\mathbf{x}, \mathbf{z}) \boldsymbol{\zeta} - 2 g_{syn} \boldsymbol{E} \times \boldsymbol{\xi} + O(\boldsymbol{\xi}^2), \\ \dot{\boldsymbol{\zeta}} &= D_{\mathbf{x}} \boldsymbol{G}(\mathbf{x}, \mathbf{z}) \boldsymbol{\xi} + D_{\mathbf{z}} \boldsymbol{G}(\mathbf{x}, \mathbf{z}) \boldsymbol{\zeta} + O(\boldsymbol{\xi}^2),\end{aligned} \tag{11}$$

where $\boldsymbol{E} = e_{ij}$ is a 2×2 matrix with $e_{11} = 1$ and 0 otherwise. Replacing the equations for $\boldsymbol{F}$ and $\boldsymbol{G}$, it yields the variational equation for the synchronous states:

$$\begin{aligned}\dot{\xi} &= (2ax - 3x^2 - 2g_{syn})\xi + \eta - \zeta, \\ \dot{\eta} &= 2bx\xi - \eta, \\ \dot{\zeta} &= \mu[s\xi - \zeta].\end{aligned} \tag{12}$$

To determine whether the synchronized states are stable we analyze the conditional transversal exponents of Eq. (12). The two largest ones are shown in Fig 1. As the coupling increases,

the two neurons undergo a transition to CS. However, CS is preceeded first by a transition to complete synchronization in the slow time-scale (burst) for g_{syn} =0.44 and then by a transition to CS in the fast time-scale (spikes), for g_{syn} =0.47.

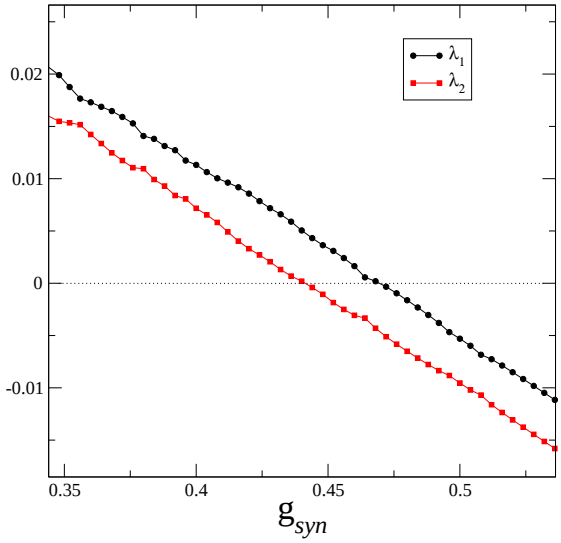

Fig. 1. The two largest transversal conditional exponents show that in the neurons coupled via electrical synapse, the burstings become synchronous for a $g_{syn} \approx 0.44$, a value smaller than when CS takes place, $g_{syn} \approx 0.47$, and the spikings become also synchronous.

The synchronization analysis can be done by means of the localized sets. We define the event occurrence to be the crossing of the membrane potential with the threshold $x_{th} = 1.0$. Note that the event is defined in the fast time scale.

The perturbations of the synchronized solutions diverge from zero at $g_{syn} = 0.1$ [Fig. 2(a-c)]; there is no synchronization. As we increase the coupling to $g_{syn} = 0.465$ the slow scale undergoes a transition to CS, while the other perturbations remain away from 0 [Fig. 2(d,e)]. The analysis of the set $\mathcal{D}$ shows that there is phase synchronization in the fast time scale [Fig. 2(f)]. So information can be transmitted at a low rate of errors in the fast scale, while in the slow scale information can be transmitted without errors. Finally, at $g_{syn} = 0.55$ all the perturbations decay to zero. Hence, the two neurons are synchronous in both time-scales [Fig. 2(g,h)]. Since there is complete synchronization in the spike scale the set $\mathcal{D}$ converges to a point.

For bursting complete synchronization [Fig. 2(d,f)] there are no positive transverse exponents corresponding to the slow synchronization manifold. If we had constructed the sets $\mathcal{D}$ with an event defined by the bursts, the set $\mathcal{D}$ would converge to a point, showing that the two oscillators are complete synchronized in this time-scale. The localized sets would show that no error in the information transmission is due to the bursts. Thus, information can be carried by the bursts without errors.

Equation (4) estimates the information exchange for the system as a whole, both time-scales. Whenever the synchronous behavior is stable in both scales the term $\sum \lambda_{\perp}^{+}$ vanishes. Hence, Eq. (4) reads $I(\mathbf{x_1 x_2}) = \sum \lambda_{\parallel}^{+} \approx H_{KS}$, where H_{KS} stands for the Kolmogorov-Sinai entropy of the coupled neurons. For burst synchronization, a positive transversal exponent associated with the spike dynamics will generate errors in the information transmission. We can estimate the amount of errors either by the localized set or by computing $\lambda_{\perp}^{max}$ the largest

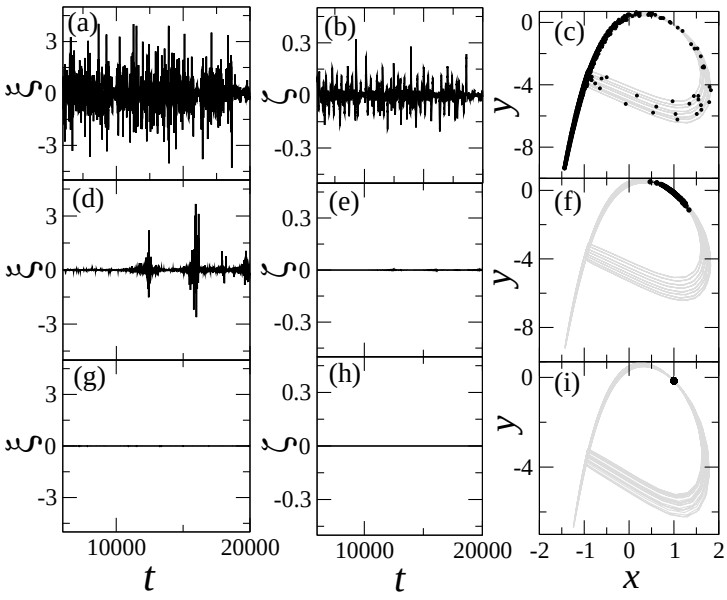

Fig. 2. The behavior of the perturbations of the synchronized solution as a function of the coupling strength. We construct the sets $\mathcal{D}$; the event occurrence is given by the crossing of the membrane potential, the x variable, with the threshold $x_{th} = 1.0$. In (a,b) for $g_{syn} = 0$, the perturbations are large, and the set $\mathcal{D}$ is not localized (c), which means that there is no synchronization. For $g_{syn} = 0.47$ there is no complete synchronization in the fast time scale (d), while complete synchronization in the slow time scale is present (e). However, the set $\mathcal{D}$ is localized (f). Since we are using the event at the spiking scale, the localization of the set $\mathcal{D}$ means that there is PS in the spikes. Finally, for $g_{syn} = 0.55$ both time-scales synchronize. The perturbations converge to zero (g,h) and the set $\mathcal{D}$ converge to a point (i), meaning CS.

transverse Lyapunov exponent, Fig. 1. Either ways, we obtain the same results.$\sum \lambda_{\|}^{+}$ can be estimated by the largest Lyapunov exponent $\lambda^{max} \approx 0.018$. Therefore, $I(\mathbf{x_1 x_2}) \approx \lambda^{max} - \lambda_{\perp}^{max}$, where $\lambda_{\perp}^{max} \approx 0.004$. Since $\lambda_{\perp}^{max} \ll \lambda^{max}$, we obtain $I(\mathbf{x_1 x_2}) \approx \lambda^{max} \approx H_{KS}$. Therefore, we conclude that, when the neurons present only burst synchronization, the most appropriate scale to retrieve information is the bursting scale. However, information could also be retrieved, with a low probability of errors, from the spiking scale

The synchronization of distinct time scales for electrically coupled neurons has been recently analyzed [34]. In particular, it is also possible to carry out an analytical estimation for the threshold for the burst synchronization onset, see [34] for a detailed analysis.

4 Chemical Synapses

We first consider a pulsatile function modeled as a static sigmoidal nonlinear input-output function with a threshold and a saturation parameters. Afterwards, we shall consider other coupling functions. For now, we have $\mathbf{H}(\mathbf{x}_i, \mathbf{x}_j) = [(x_i - V_s)\Gamma(x_j), 0]^T$. The coupling matrix is the matrix $\boldsymbol{E}$ defined in the previous section. The reversal potential $V_s > x_i(t)$ for any x_i implies that the synapse is excitatory with $V_s = 2.0$. The synaptic coupling function is modeled by the sigmoidal function

$$\Gamma(x_j) = \frac{1}{1 + e^{-\lambda(x_j - \Theta_s)}} \tag{13}$$

This coupling function is also called fast threshold modulation [48]. The parameters are $\lambda = 10$, and $\Theta_s = -0.25$, chosen in such a way that every spike within a single neuron burst can reach the threshold. In this case, the synchronized solution takes the form

$$\begin{aligned} \dot{x} &= ax^2 - x^3 + y - z - g_{syn}(x - V_s)\Gamma(x), \\ \dot{y} &= 1 + bx^2 - y, \\ \dot{z} &= \mu[s(x - x_0) - z]. \end{aligned} \tag{14}$$

Considering $\boldsymbol{\xi} = \mathbf{x}_1 - \mathbf{x}_2 = (\xi_i, \eta_i)^T$, and $\boldsymbol{\zeta} = \mathbf{z}_1 - \mathbf{z}_2 = \zeta_i$. The only variable with a non-trivial derivation is ξ. All the others are easily obtained by calculating the Jacobian of the $\boldsymbol{F}$ and $\boldsymbol{G}$. Writing $\mathbf{x}_1 = \boldsymbol{\xi} + \mathbf{x}_2$, we arrived at $\dot{\xi} = \partial_x f\xi + \partial_y f\eta + \partial_z f\zeta + g_{syn}[\xi\Gamma(x_2) - \xi(x_2 - V)\Gamma'(x_2)]$. Considering that $\mathbf{x}_2 = \mathbf{x}_1$, we have the variational equations

$$\begin{aligned} \dot{\xi} &= (2ax - 3x^2)\xi + \eta - \zeta - g_{syn}\Gamma(x)\xi + g_{syn}(x - V_s)\Gamma'(x)\xi \\ \dot{\eta} &= 2bx\xi - \eta, \\ \dot{\zeta} &= \mu[s\xi - \zeta], \end{aligned} \tag{15}$$

where

$$\Gamma'(x) = \frac{\lambda e^{-\lambda(x-\Theta_s)}}{\left[1 + e^{-\lambda(x-\Theta_s)}\right]^2}, \tag{16}$$

with the intrinsic current $I_{ext} = 3.2$. For the studied parameters, and a coupling slightly bigger than the one at which CS is obtained, the neurons undergo a transition to rest state and present no longer a dynamical behavior.

To determine whether the synchronized states are stable, we analyze the Lyapunov exponents of the variational Eq. (15), the transversal conditional exponents. Two of those are shown in Fig. 3. As the coupling increases, similarly to the electrical coupling, first the bursting scale becomes synchronous followed by CS when also the spiking scale becomes synchronous. The information analysis is similar to the one made in the previous section.

5 Excitatory Networks of Identical Neurons

We consider a network formed by HR neurons. The theory developed in Ref. [49] predicts that for networks of identical neurons, where all neurons receive the same number of synaptic inputs k, the onset of CS is given by:

$$g_{syn} = \frac{g_{syn}^{n=2}}{k}, \tag{17}$$

where $g_{syn}^{n=2}$ is the coupling strength needed to achieve CS between two neurons. For a network randomly connected of 9 HR neurons, where every neuron receives the same number $k = 3$ of inputs, CS sets in at $\bar{g}_{syn} \approx 0.425$.

Note that, even though the isolated neurons are identical, before the onset of PS they have a different dynamical behavior due to the coupling. So, the synchronization manifold does not exist and there is no sense in trying to make the analysis in order to identify separately when the different time scales synchronize. We found, numerically by the observations of the localized sets, that PS in the whole network is already achieved at $g_{syn}^* \approx 0.36$. Clusters of PS, however, appear for a much smaller value of the coupling strength, actually at $g_{syn} \approx 0.03$.

Clusters of PS inside the network may offer a suitable environment for information exchanging. Each one can be regarded as a channel of communication, since they possess different frequencies, each channel of communication operates in different bandwidths.

Such clusters of phase synchronized neurons are rather suitable for communication exchanging. They provide a multichannel communication, that is, one can integrate a large number of

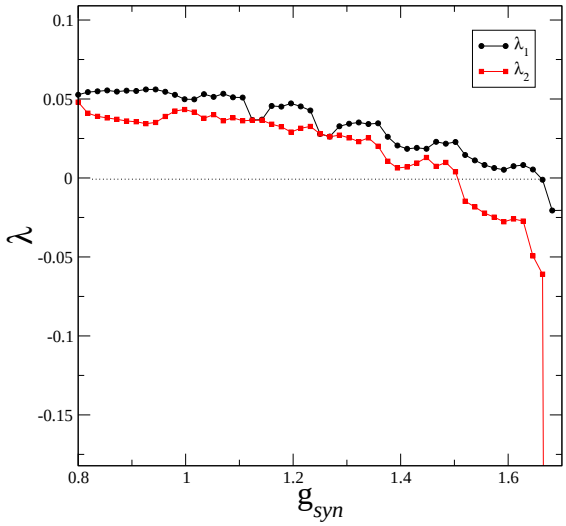

Fig. 3. The two largest transversal conditional exponents show that also in the neurons coupled via chemical synapse, the bursting become synchronous for a g_{syn} smaller than when CS takes place, and the spiking become also synchronous.

neurons (chaotic oscillators) into a single communication system, and information can arrive simultaneously at different places of the network. This scenario may have applications to digital communication [32,50], and it may also guide us towards a better understanding of information processing in real neural networks [12,51].

6 Mismatches in the Synaptic Strength

Still holding the constraint of the same number of input for all neurons, we can study the influence of the mismatches in the synaptic strength. So, instead of considering a constant strength, we rather consider it with a dependence on the space (network elements). For the mismatch situation, we may write: $g_{syn}(i,j) = g_{syn} + \theta_{ij}$, where θ_{ij} is the mismatch parameter. If $g_{syn} \neq 0$, we can also write: $g_{syn}(i,j) = g_{syn}(1 + \theta_{ij}/g_{syn})$, introducing $\beta_{ij} = \theta_{ij}/g_{syn}$. Therefore, Eq. (8) takes the form

$$\begin{aligned} \dot{\mathbf{x}}_i &= \boldsymbol{F}(\mathbf{x}_i, \mathbf{z}_i) + g_{syn} \sum_j (1 + \beta_{ij}) c_{ij} \mathbf{H}(\mathbf{x}_i, \mathbf{x}_j), \\ \dot{\mathbf{z}}_i &= \mu \boldsymbol{G}(\mathbf{x}, \mathbf{z}). \end{aligned} \tag{18}$$

where c_{ij} is the coupling matrix. Our numerical analysis has shown that for suitable mismatches in the synapses strengths one can improve the appearance of clusters in the network. For example, considering the last example with the HR network clusters appear at $g_{syn} \approx 0.03$. For a θ_{ij} given by a Gaussian distribution with variance equal to 0.01 clusters of burst phase synchronization appear even for $g_{syn}(i,j) = \theta_{ij}$, which means that $g_{syn} = 0$.

A theoretical analysis of this synaptic mismatch procedure can be done not only for the case where the number of input is constant, but also for a general network. Eq. (19) has been consider by Qi et al. [52]. Their analysis show that some clusters of completely synchronous neurons may appear for neurons that have the same $l_i = \sum_j (1 + \beta_{ij}) c_{ij}$. The equation corresponding to the

synchronized motion, $\mathbf{x}_i = \mathbf{x}$ and $\mathbf{y}_i = \mathbf{y}$, is given by

$$\begin{aligned} \dot{\mathbf{x}} &= \boldsymbol{F}(\mathbf{x}, \mathbf{z}) + g_{syn} l \mathbf{H}(\mathbf{x}, \mathbf{x}), \\ \dot{\mathbf{z}} &= \mu \boldsymbol{G}(\mathbf{x}, \mathbf{z}). \end{aligned} \tag{19}$$

The analysis carried out in Ref. [52] shows that this equation admits a stable synchronous solution if $g_{syn} l$ exceeds a threshold, which is network-structure free, in other words, it does not depend on the network topology. Furthermore, if the neurons have different l_i complete synchronization is no longer possible, however, the neurons may present burst synchronization. So, if one wants to induce the appearance of clusters of synchronous neurons one may use a mismatch in the synaptic strength. Each cluster will be formed by the neurons that possess the same l_i.

7 Networks of Non-identical Neurons

In this section, we study the onset of synchronization in a network of spiking/bursting non-identical neurons. We couple the neurons via an excitatory synapse. Since the neuron parameters mismatch, CS is no longer possible, but rather PS. We detect PS and estimate the information capacity between neurons in this type of network by means of the localized sets.

We also use a more realistic 4-dimensional HR model [53,47]. The neurons are described by a set of four coupled differential equations:

$$\begin{aligned} \dot{x}_i &= a y_i + b x_i^2 - c x_i^3 - d z_i + I_i + g_{syn} \mathbf{C} \mathbf{I}_{syn}(\mathbf{x}), \\ \dot{y}_i &= e - y_i + f x_i^2 - g w_i, \\ \dot{z}_i &= \mu(-z_i + R(x_i + H)), \\ \dot{w}_i &= \nu(-k w_i + r(y_i + l)), \end{aligned} \tag{20}$$

where x_i represents the membrane potential of the neuron $\mathcal{N}_i$, y_i is associated with fast currents exchange and (z_i, w_i) with slow currents dynamics, $\mathbf{I}_{syn}(\mathbf{x}) = (I_{syn}(x_1), I_{syn}(x_2), \ldots, I_{syn}(x_N))$ is the synaptic input vector and $I_{syn}(x_j)$ is the synaptic current that neurons $\mathcal{N}_j$ (post-synaptic) injects in $\mathcal{N}_i$ (pre-synaptic), and $\mathbf{C} = \{c_{ij}\}$ is the $N \times N$ connectivity matrix where $c_{ij} = 1$ if neuron $\mathcal{N}_j$ is connected to neuron $\mathcal{N}_i$, and $c_{ij} = 0$, otherwise, with $j \neq i$. This model has been shown to be realistic, since it reproduces the membrane potential of biological neurons [54], and it is able to replace a biological neuron in a damaged biological network, restoring its natural functional activity [55]. It also reproduces a series of collective behaviors observed in a living neural network [53]. The parameters of the model are the same as in Ref. [53], but the intrinsical current I_i. We change I_i in order to obtain a spiking/bursting behavior and we use it as a mismatch parameter.

The chemical synapses [56] are modeled by:

$$\begin{aligned} I_{syn}(x_j) &= S(t)\,(x_{rev} - x_j)\,, \\ [1 - S_\infty(x_i)]\,\tau \dot{S}(t) &= S_\infty(x_i) - S(t), \end{aligned} \tag{21}$$

where x_j is the post-synaptic neuron, x_{rev} is the reversal potential for the synapse, and τ is the time-scale governing the receptor binding. S_∞ is given by:

$$S_\infty(x_i) = \begin{cases} tanh\left(\frac{x_i - x_{th}}{x_{slope}}\right), & \text{if} \quad x_i > x_{th} \\ 0 & \text{otherwise} \end{cases} \tag{22}$$

The synapse parameters are $x_{th} = -0.80$, $x_{slope} = 1.00$, $x_{rev} = -1.58$. They are chosen in such a way to obtain an inhibitory effect in the chemical synapse.

We consider a network of 100 non-identical HR neurons, regarded as $\mathcal{N}_i$ where $i \in [1, \ldots, 100]$, connected via excitatory chemical synapses. The mismatch parameter is the intrinsic current I_i.

For $I_i = 3.12$, the HR neuron presents a chaotic spiking/bursting behavior, the same found in biological neurons. We introduce mismatches around this value for all the neurons within the network. Thus, given a random number η_i uniformly distributed within the interval $[-0.05, 0.05]$, we set $I_i = 3.12 + \eta_i$. To obtain an excitatory synaptic effect we use $x_{rev} \geq x_i(t)$, which means that the pre-synaptic neuron always injects a positive current in the post-synaptic one. Since the largest spike amplitude is around 1.9, we set $x_{rev} = 2.0$.

Our network is a homogeneous random network, i.e. all neurons receive the same number k of connections, namely $k = 30$. We constrain g_{syn} to be equal to all neurons. We identify the amount of phase synchronous neurons by analyzing whether the sets $\mathcal{D}_i$ are localized. An example is presented in Fig. 4. We choose three neurons out of the 100 neurons forming the network. Their membrane potential is depicted in Fig. 4 (a), we name these neurons as $1, 2$ and 3. Only the neurons 2 and 3 present PS. Therefore, the set $\mathcal{D}_{12}$ (the subscript means that the set is constructed considering the neurons 1 and 2) is not localized, Fig. 4(b). Whereas the set $\mathcal{D}_{23}$ is localized, Fig. 4(c).

The onset of PS in the whole network takes place at $g^*_{syn} \approx 0.0085$; so all neurons become

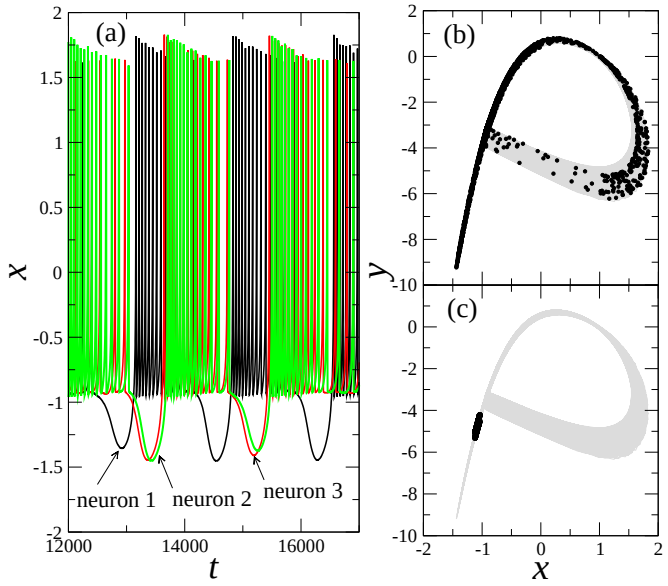

Fig. 4. Time series of three neurons of a network of 100 neurons. Neurons 2 and 3 present PS between themselves but not with neuron 1 (a). The analysis of the sets $\mathcal{D}$ confirms this statement. In (b) we construct the set $\mathcal{D}$ between neurons 1 and 2. The set spreads over the attractor, and few information can flow between these two neurons. In (c) we show the set $\mathcal{D}$ constructed with the neurons 2 and 3, which is localized.

phase synchronized. As the synapse strength crosses another threshold, $\tilde{g}_{syn} \approx 0.45$, the neurons undergo a transition to the rest state, no longer presenting an oscillatory behavior. Clusters of PS appear for $\bar{g}_{syn} \ll g^*_{syn}$. In fact, right at $g_{syn} \approx 0.0005$, PS clusters appear [Fig. 5(a)], then, as we increase the coupling strength more and more clusters appear, see Fig. 5(b-d). Again, the clusters are identified by analyzing the localized sets. These clusters seem to be robust under small perturbations.

An important characteristic of the network is the mean field behavior. The emergence of a collective behavior enhances a mean field that captures the dynamics of the neuron network. Such a behavior can be problematic and might lead to the appearance of some diseases [12]. In this situation a massive population of neurons behaves in a similar fashion not allowing a

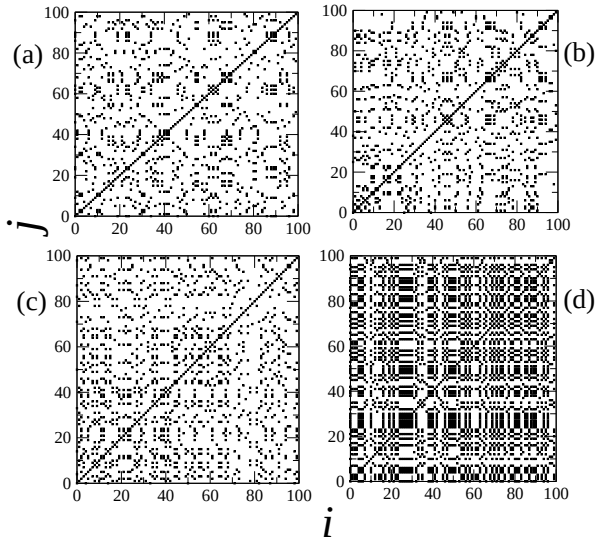

Fig. 5. Clusters of PS for a random homogenous network of 100 non-identical HR neurons. A point i and j indicates that the neuron i presents PS with neuron j. In (a) for $g_{syn} = 0.0005$ approximately 25 neurons are phase synchronized. In (b-d) we increase the coupling strength $g_{syn} = 0.001$, 0.002, and 0.003 respectively.

dynamical behavior apart from the collective one. And if the characteristic of an information signal differs from the mean field behavior, for example having a different frequency, it will hardly be spread through the network.

The appearance of PS clusters might be a special characteristic in such neural networks. The neurons can transmit information in a multichannel way (through many oscillators) still displaying a low mean field behavior. In Fig. 6(a) for $g_{syn} = 0.0001$ there is no synchronization among the neurons within the network, and the mean field presents no dynamics, but a noise-like signal, fluctuating around the mean value. As the clusters of PS appear, the mean field is still very small. Then, when approximately 20% of the network is synchronized a field behavior with a low frequency oscillation takes place [Fig. 6(b)].

The more phase synchronized neurons the higher the mean field becomes. As an example, when approximately 35% of the neurons present PS, the mean field already captures the dynamics of the phase synchronized bursts [Fig. 6(c)]. For strong enough coupling, many clusters of neurons with phase synchronized spikes appear, which also enhances a positive mean field behavior in the fast time-scale [Fig. 6(d)].

The clusters do not always have the same frequency, which means that in addition to the multichannel communication provided by the clusters, we can also transmit information in more than one bandwidth. To characterize the bandwidths within the network we analyze the variance in the average bursting time of the neurons. Since only the bursting scale is synchronized, we are just interested in the average bursting time, which can be straightforwardly estimated with a fast Fourier transformation FFT [57]. So, given the neuron $\mathcal{N}_j$, we label its bursting average time by $\langle T_j \rangle$. Then, we compute the variance of the average time on the ensemble of neurons. For this, we first introduce the average time of the whole network, which is given by:

$$\zeta = \frac{1}{n} \sum_{j=1}^{n} \langle T_j \rangle. \tag{23}$$

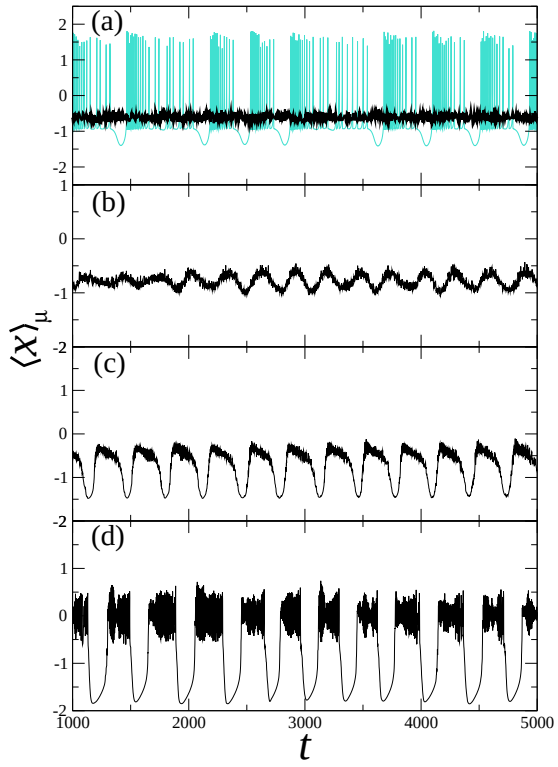

Fig. 6. Mean field behavior for the network, calculated by averaging the membrane potential x. For $g_{syn} = 0.0001$, all the neurons are not phase synchronized, which generates a steady mean field with fluctuations. For $g = 0.0005$ clusters of PS appear. Even though the clusters have different frequencies, the mean field presents a slow frequency (b). As we increase the synaptic strength $g_{syn} = 0.003$ more clusters appears enhancing a mean field that captures the dynamics of the burst scale (c). For strong enough coupling, the clusters of neurons with phase synchronized spikes appear followed by a dynamical behavior of the mean field also on the fast time-scale (d).

Thus, the variance of the average time on the ensemble of neurons is readily written as:

$$\sigma^2 = \frac{1}{n}\sum_{j=1}^{n}(\langle T_j \rangle - \zeta)^2. \tag{24}$$

So, σ indicates how diverse are the bandwidths. The result $\sigma^2 \times g_{syn}$ is depicted in Fig. 7. As one can see in Fig 7, when the first clusters appear for $g_{syn} \approx 0.0005$, the network becomes more non-coherent, i.e. σ is increased, and clusters of different frequencies take place. A further increasing of g_{syn} causes the appearance of more synchronized neurons and a reduction of σ. At $g_{syn} = 0.0085$, the whole network undergoes a transition to burst PS, therefore $\sigma = 0$.

8 Conclusions

We analyze the effect of synchronization in networks of chemically coupled multi-time-scales (spiking-bursting) neurons on the information transmission exchange process. We show that synchronization occurs first in the slow time scale (burst) and then in the fast time scale (spike), however, the information can be transmitted with a low probability of errors in both scales at the onset of burst synchronization. Furthermore, we show that for networks of non-identical multi-time-scales neurons complete, synchronization can be no longer achieved, but

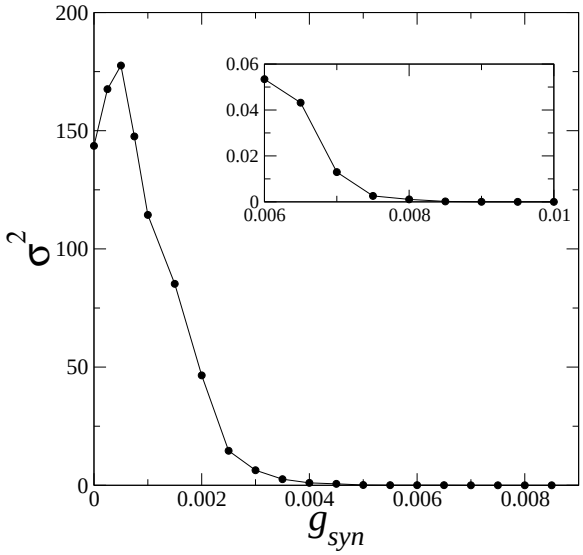

Fig. 7. Variance of the bandwidths within the network. For $g_{syn} \approx 0.0085$ the whole network undergoes a transition to PS.

rather the neurons may present burst phase synchronization. Our analysis shows that clusters of burst phase synchronized neurons are very likely to appear in a network before the onset of burst phase synchronization in the whole network.

Acknowledgment We thank the Helmholtz Center for Brain and Mind Dynamics (TP and JK) for financial support. TP thanks the Max-Planck-Institut für Physik Komplexer Systeme for the hospitality and pleasant stay, when the manuscript was being revised.

References

1. M. Steriade and R. R. Llinas, Physiol. Rev. **68**, 649 (1988).
2. S. M. Sherman and C. Kock, Exp. Brain Res. **63**, 1 (1986).
3. E. R. Kandel, J.H. Schwartz, and T.M. Jessel, *Principles of neural science* fourth editon (Mc. Graw Hill, 2000).
4. W. Schultz, J. Neurophysiol. **80**, 1 (1998).
5. A. S. Freeman, L. T. Meltzer, and B. S. Bunney, Life Sci. **36**, 1983 (1985).
6. A. A. Grace and B. S. Bunney, Neuroscience **10**, 2877 (1984).
7. E. Rodriguez, N. George, J. P. Lachaux, *et al.*, Nature **397**, 430 (1999).
8. M. Stopfer and G. Laurent, Nature **402**, 664 (1999).
9. P. Fries, J. H. Reynolds, A. E. Rorie, *et al.*, Science **291**, 1560 (2001).
10. T. Seidenbecher, T. Rao Laxmi, O. Stork, *et al.*, Science **301**, 846 (2003).
11. P. Tass, M.G. Rosenblum, J.Weule, *et al.*, Phys. Rev. Lett. **81**, 3291 (1998).
12. F. Mormann, T. Kreuz, R. G. Andrzejak, *et al.* Epilepsy Research **53**, 173 (2003).
13. A. Borst and F.E. Theunissen, Nature Neurosci. **2**, 947 (1999)
14. J.J. Eggermont, Neurosc. & Biobehavi. Rev. **22**, 355 (1998).
15. A. Catteneo, L. Maffei, C. Morrone, Proc. Royal Soc. London B **212**, 279 (1981).
16. S. Spinoza, *Ethics demonstrated in geometrical order*; Part I prop. iv. (MTSU Philosophy Web-Works Hypertext Edition, 1997)
17. N. F. Rulkov, Phys. Rev. Lett. **86**, 183 (2001).
18. H. Fujisika and T. Yamada, Progr. Theoret. Phys. **69**, 32 (1983).
19. L. M. Pecora and T. Carrol, Phys. Rev. Lett. **64**, 821 (1990).
20. L. M. Pecora and T. Carrol, Phys. Rev. Lett. **80**, 2109 (1998).

21. S. Strogatz, *Sync: The Emerging Science of Spontaneous Order* (Hyperion, 2003).
22. S. Boccaletti, J. Kurths, G. Osipov, *et al.*, Phys. Rep. **366** 1 (2002); J. Kurths, S. Boccaletti, C. Grebogi, *et al.* Chaos **13**, 126 (2003).
23. A. S. Pikovsky, M. G. Rosenblum, and J. Kurths, *Synchronization: A Universal Concept in Nonlinear Sciences*, (Cambridge University Press, 2001).
24. I. Leyva, E. Allaria, S. Boccaletti, *et al.*, Phys. Rev. E **68**, 066209 (2003).
25. I. Fischer, Y. Liu, and P. Davis, Phys. Rev. A **62**, 011801 (2000).
26. M. G. Rosenblum, A. S. Pikovsky, and J. Kurths, Phys. Rev. Lett. **76**, 1804 (1996); A. S. Pikovsky, M.G. Rosenblum, and J. Kurths, Physica D. **76**, 1804 (1997).
27. U. Parlitz, L. Junge, W. Lauterborn, *et al.*, Phys. Rev. E **54**, 2115 (1996).
28. M. S. Baptista, T. Pereira, J. C. Sartorelli, *et al.*, Phys. Rev. E **67**, 056212 (2003).
29. I. Z. Kiss and J. L. Hudson, Phys. Rev. E, **64**, 046215 (2001).
30. C. M. Ticos, E. Rosa Jr., W. B. Pardo, *et al.*, Phys. Rev. Lett. **85**, 2929 (2000).
31. S. Hayes, C. Grebogi, E. Ott, *et al.* Phys. Rev. Lett. **73**, 1781 (1994).
32. T. Yalçinkaya and Y. C. Lai, Phys. Rev. Lett. **79**, 3885 (1997).
33. G. V. Osipov, M. V. Ivanchenko, J. Kurths, *et al.*, Phys. Rev. E **71**, 056209 (2005).
34. M. Dhamala, V. K. Jirsa, and M. Ding, Phys. Rev. Lett. **92**, 028101 (2004).
35. R. Ellison, V. Gardner, J. Lepak, *et al.*, Inter. Jour. Bif. Chaos **15**, 2283 (2005); W.J. Freeman and J.M. Barrie, Jour. Neurophys. **84**, 1266 (2000).
36. P. A. Tass, T. Fieseler, J. Dammers, *et al.*, Phys. Rev. Lett. **90**, 088101 (2003).
37. K. Josić and M. Beck, Chaos **13**, 247 (2003); K. Josić and D. J. Mar, Phys. Rev. E **64**, 056234 (2001).
38. T. Pereira, M. S. Baptista, and J. Kurths, Phys. Lett. A **362**, 159 (2007).
39. If the set $\mathcal{D}$ is a subset of Φ, we say that $\mathcal{D}$ localized (with respect to Φ) if there is a cross section Ψ and a neighborhood Λ of Ψ, such that $\mathcal{D} \cup \Lambda = \emptyset$. In particular, for practical detections, one may check whether $\mathcal{D}$ is localized, by the following technique. If there is PS, for $\mathbf{y} \in \mathcal{D}$ it exists infinitely many $\mathbf{x} \in \Lambda$ such that $\mathbf{y} \cap B_\ell(\mathbf{x}) = \emptyset$, where $B_\ell(\mathbf{x})$ is an open ball of radius ℓ centered at the point $\mathbf{x}$, and ℓ is small. Then, we may vary $\mathbf{y}, \mathbf{x}$ (one may take $\mathbf{x}$ to be an arbitrary point of the attractor) and ℓ, to determine whether $\mathcal{D}$ is localized.
40. M. S. Baptista, T. Pereira, J. Kurths, Physica D **216**, 260 (2006).
41. M. S. Baptista, T. Pereira, J. C. Sartorelli, *et al.*, Physica **D 212** 216 (2005).
42. T. Pereira, M. S. Baptista, and J. Kurths, Europhys. Lett. **77**, 40006 (2007).
43. T. Pereira, M. S. Baptista, and J. Kurths, Phys. Rev. E **75**, 026216 (2007).
44. T. Pereira, M. S. Baptista, M. B. Reyes, *et al.*, *Onset of Phase Synchronization in Neurons Connected by Chemical Synapses*, to appear in IJBC.
45. C. E. Shannon, The Bell Syst. Tech. Jour. **27**, 623 (1948).
46. M. S. Baptista and J. Kurths, Phys. Rev. **E 72**, 045202R (2005).
47. J. L. Hindmarsh and R. M. Rose, Proc. R. Soc. Lond. B. **221**, 87 (1984); J. L. Hindmarsh and R. M. Rose, Nature **296**, 162 (1982).
48. H. J. Sommers, A. Crisanti, H. Sompolinsky, *et al.*, Phys. Rev. Lett. **60**, 1895 (1988).
49. I. Belykh, E. Lange, and M. Hasler, Phys. Rev. Lett **94**, 188101 (2003).
50. S. Hayes, C. Grebogi, E. Ott, *et al.*, Phys. Rev. Lett. **73**, 1781 (1994).
51. R. Borisyuk, G Borisyuk, and Y. Kazanovich, Behavior and Brain Sc. **21**, 833 (1998).
52. G. X. Qi, H. B. Huang, H. J. Wang, *et al.*, Europhys. Lett. **74**, 733 (2006).
53. R. D. Pinto, P. Varona, A. R. Volkovskii, *et al.*, Phys. Rev. E **62**, 2644 (2000).
54. S. W. Johnson, V. Seutin, and R. A. North, Science **58**, 665 (1992).
55. C. Mulle, A. Madariaga, and M. Deschenes, J. Neurosci. **6**, 2134 (1986).
56. A. Destexhe, Z. F. Mainen, and T. J. Sejnowski, Neural Comput. **6**, 14 (1994); A. A. Sharp, F. K. Skinner, and E. Narder, J. Neurophysiol. **76**, 867 (1996).
57. I. N. Sneddon, *Fourier Transforms*. (Dover, 1995).